Biosensors and Bioelectronics 24 (2009) 3425–3429

Biosensors and Bioelectronics

journal homepage: www.elsevier.com/locate/bios

New insights for using self-assembly materials to improve the detection stability in label-free DNA-chip and immuno-sensors☆

Sandro Carrara[a,*], Luca Benini[b], Vijayender Bhalla[a], Claudio Stagni[a,b], Anna Ferretti[a], Andrea Cavallini[b], Bruno Riccò[b], Bruno Samorì[a]

[a] Biochemistry Department "G.Moruzzi", University of Bologna, Bologna, Italy
[b] Department DEIS, University of Bologna, Bologna, Italy

ARTICLE INFO

Article history:
Received 12 September 2008
Received in revised form 31 October 2008
Accepted 5 November 2008
Available online 27 November 2008

Keywords:
DNA-chip
Immuno-sensors
Capacitance detection
Alkanethiols
Ethylene–glycol molecules
Ion layering
AFM
QCM

ABSTRACT

This paper examines reliable advancements in low-cost DNA- and immuno-chips. Capacitance detection was successfully chosen to develop label-free bio-chips. Probe immobilization was rigorously investigated in order to obtain reliable capacitance measurements. Protein probes immobilized by using usual alkanethiols or thiolated ssDNA probes directly immobilized on gold do not allow sufficient stable capacitance measurements. New alkanethiols improved with ethylene–glycol function are shown in this paper to be more suitable materials for capacitive bio-chip development. Atomic Force Microscopy, Quartz Crystal Microbalance, and Capacitance Measurements were used to demonstrate that ethylene–glycol alkanethiols allow high time stability, smaller errors in detection, and improved ideal behaviour of the sensing surfaces. Measured capacitance is in the range of 8–11 nF/mm^2 for antibody layers and close to 6 nF/mm^2 for DNA probes. It is in the range of 10–12 nF/mm^2 and of 4–6 nF/mm^2 for antigen and DNA detection, respectively. The percentage error in detection is highly improved and it is in the range of 11–37% and of 0,23–0,82% for antigen and DNA, respectively. The reproducibility is also improved and it is close to 0,44% for single spot measurements on ethylene–glycol alkanethiols. A molecular theory attributing these improvements to water molecules strongly coordinated by ethylene–glycol functional groups and to solution ions not entering into probe films is finally proposed.

1. Introduction

Label-free detection is a suitable technique delivering fast response and low-cost applications in point-of-care devices. Among them, capacitance transduction attracts researchers since it is easily integrated into CMOS technology. It was initially proposed for immuno-sensors development (Mirsky et al., 1997) and different alkyl thiols were tested for antibody immobilization (Riepl et al., 1999). It was proposed for the detection of gonadotropins (Berggren and Johansson, 1997), interleukins (Berggren et al., 1998), heavy metals (Corbisier et al., 1999), and DNA hybridization (Berggren et al., 1999). The achieved detection limit has been found in the femtomolar range (Bontidean et al., 2003). Detection of DNA was successfully demonstrated onto gold (Guiducci et al., 2004), normal silicon (Balasubramanian et al., 2005) and macroporus silicon (Betty et al., 2004) electrodes. It was also verified by using PNA (Peptide Nucleic Acid) probes (Macanovic et al., 2004). Recently, fully integrated CMOS bio-chips were developed for DNA detection (Stagni et al., 2006, 2007). Some good reviews describing details of this progress were published in the recent years (Berggren et al., 2001; Gabig-Ciminska, 2006; Daniels and Pourmand, 2007). However, despite this large effort in demonstrating the different possible applications of label-free impedance biosensors, the published data are not reliable enough for point-of-care developments. Published data usually present a large time drift (Riepl et al., 1999; Stagni et al., 2006), very large standard deviation (Berggren et al., 2001; Stagni et al., 2007), largely scattered data points (Mirsky et al., 1997; Berggren et al., 1999), poor reproducibility between electrodes (Berggren et al., 1998), and interfacial behaviour too far from that of an ideal capacitor (Carrara et al., 2007). Moreover, specificity is not very high (Berggren et al., 1998) and signals from non-specific molecules are often present (Stagni et al., 2006, 2007). The aim of this paper is to present improvements in terms of measurement stability and reproducibility by using new self-assembly strategies. The work is based on ethylene–glycol alkanethiols invented by George M. Whitesides. They were developed to decrease the interference of non-specific protein binding in Surface Plasmon Resonance biosensors (Ostumi et al., 1999; Horan et al., 1999; Lahiri et al., 1999). In the present article, we demonstrate that ethylene–glycol

☆ This article is a part of the special issue "Biosensors 2008".

* Corresponding author at: Swiss Federal Institute of Technology - Lausanne EPFL IC ISIM LSI1 - INF 333 (Bâtiment INF), Station 14, CH-1015 Lausanne, Switzerland. Tel.: +41 21 693 678; fax: +41 78 7938837.
E-mail address: sandro.carrara@epfl.ch (S. Carrara).
URL: http://www.si2.epfl.ch/ scarrara/ (S. Carrara).

0956-5663/$ – see front matter © 2008 Elsevier B.V. All rights reserved.
doi:10.1016/j.bios.2008.11.014

alkanethiols can be successfully used to highly improve impedance biosensors in terms of reliability of capacitance detection. Data from Atomic Force Microscopy, Quartz Crystal Microbalance, Capacitance Measurements are used to show that ethylene–glycol alkanethiols molecules eliminate data time drift and enhance the capacitive stability of DNA-chip and immuno-sensors. As a significant contribution in understanding the field of probe immobilization, we present a molecular theory attributing the stability improvement to glycolate groups of the alkanethiols monolayer.

2. Materials and Methods

2.1. Chemicals

Glycol alkanethiols differently terminated (alkanethiols terminated with $(OCH_2CH_2)_3OCH_2$—COOH; and terminated with $(OCH_2CH_2)_3$—OH) were purchased by Prochimia, Poland. 11-Mercaptoundecanoic acid, NaCl, Na_2HPO_4, KH_2PO_4, KCl, H_2O_2 50%, Standard sample of Bovine Serum Albumine (BSA), and absolute ethanol were obtained from Sigma–Aldrich. H_2SO_4, 96%, was purchased from Carlo Erba, Italy. All the chemicals were used without further purification. Antibodies against the "Squamous Cell Carcinoma Antigen" (SCCA) biomarker, and SCCA were purchased by Abnova GmbH (Heidelberg, DE).

2.2. Surfaces Preparation

DNA probe surfaces made with SH-terminated ssDNA were obtained by immobilizing oligonucleotides directly onto gold electrodes (for a schematic view, see drawing (A) reported in on-line available Supplementary file # 1). A well known protocol was used (Carrara et al., 2007). Probe surfaces made with alkanethiols were formed by using two different kinds of *Self Assembled Monolayers* (SAM) onto gold electrodes. Alkanethiols SAM without ethylene–glycol functionalization (from now on will be referred to as "non-EG-alkanethiols"-for a schematic view, see drawing (B) reported in on-line available Supplementary file # 1) were obtained from a 1 mM ethanol solution of 11-mercaptoundecanoic acid ($HS(CH_2)_{10}CO_2H$). Ethylene–glycol alkanethiols SAM (from now on "EG-alkanethiols"-for a schematic view, see drawing (C) reported in on-line available Supplementary file # 1) were prepared from an ethanol solution of $(HS(CH_2)_{11}(OCH_2CH_2)_3OH$ 1,96 mM and $HS(CH_2)_{11}(OCH_2CH_2)_3OCH_2COOH)$ 0,04 mM. The mixture was obtained with a ratio between OH-terminated and COOH-terminated thiols equal to 50:1. Both kinds of SAM were formed by using well known self-assembly procedures (Lahiri et al., 1999). Before measurements, the SAM samples were left in PBS (Phosphate Buffered Saline, water solution with 137 mM NaCl, 10 mM Phosphate, 2,7 mM KCl, at pH 7,4) buffer in dark for 24 h. This conditioning was necessary to further stabilize the capacitance measurements on the so prepared electrode chips. SAMs were formed onto template stripped gold (TSG) for AFM investigations, crystal quartz resonators for QCM investigations, and chips with interdigitated electrodes geometry for capacitance measurements. NH-terminated ssDNA probe molecules (Carrara et al., 2008) and antibodies (Lahiri et al., 1999) were immobilized onto the SAM monolayers by means of N-hydroxysuccinimide (NHS) and of Ethyl-Dimethyl-aminopropyl Carbodiimide (EDC) to form covalent bonds. Target DNA and antigen molecules were incubated following well established procedures.

2.3. Capacitance Measurements

10 μl of buffer drops were spread on top of each single sensing spot of the bio-chip for capacitance measurements. The used buffers were PBS and TE (water solution with 10 mM tris(hydroxymethyl)aminomethane, 1 mM ethylenediaminetetraacetic acid, and 0,1 M NaCl at pH 8) for measurements on proteins and DNA, respectively. Individual bio-chips were measured using an array biosensors measurement station developed in our lab. To improve the capacitance acquisition, the charge-based capacitance measurements (CBCM) (Stagni et al., 2007) technique was implemented in a PCB circuit.

2.4. AFM Measurements

Atomic force microscopy (AFM) imaging was performed in tapping mode with PointProbe nanocontact silicon probes mounted in a Nanoscope IIIa SFM system equipped with a multimode head and a type A piezoelectric scanner (Veeco, Santa Barbara, CA, USA). The images were acquired in ethanol using a 'liquid cell'. Raw images were processed only for background removal (flattening) using the microscope manufacturer's image processing software package.

2.5. QCM Mass Measurements

Functionalizations with alkanethiols, probe and target molecules were also checked using a quartz crystal microbalance (QCM). The used QCM apparatus was a home made instrument. The instrument was built by following a resonant circuit realized for the same purpose (Facci et al., 1993). Instrument calibration was done by drop casting of incremental amounts of standard Bovine Serum Albumine (BSA) onto the electrodes of crystal quartz resonators (Rickert et al., 1997). The single 5 MHz QCM crystals (catalogue code 151247–5) were purchased by ICM (International Crystal Manufacturing Co., Oklahoma City, USA).

3. Results and Discussion

3.1. Capacitance Increase in Probes Immobilization and Antigen Detection

Fig. 1 compares the behaviour of probe surfaces obtained with HS-terminated ssDNA immobilized directly onto gold and with NH-terminated ssDNA immobilized onto a film prepared by using

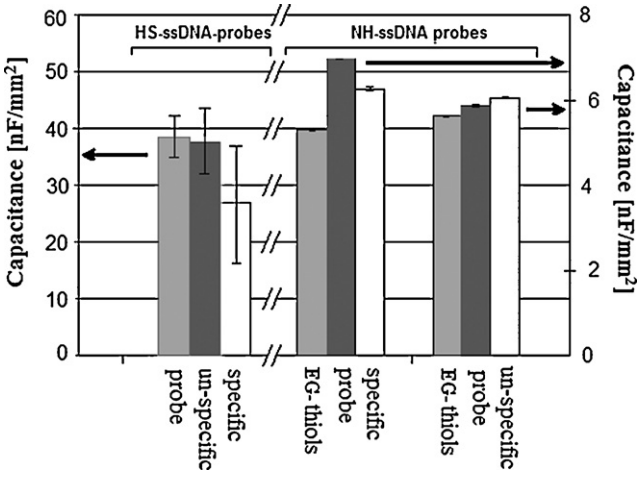

Fig. 1. Capacitance measurements acquired on probes DNA, non-specific, and specific DNA hybridized molecules. The comparison is between the usually considered immobilization technique by using HS-terminated ssDNA probes immobilized on gold (data on the left) and the new technique proposed in this paper based on NH-terminated ssDNA covalently bound to a preformed ethylene–glycol alkanethiols monolayer (data on the centre and left). The reported data errors are calculated as three times the standard deviation in measurement series acquired upon the time on the same chip spot. The errors correspond to the 99% of statistical data significance. All the measurements were carried out in TE buffer.

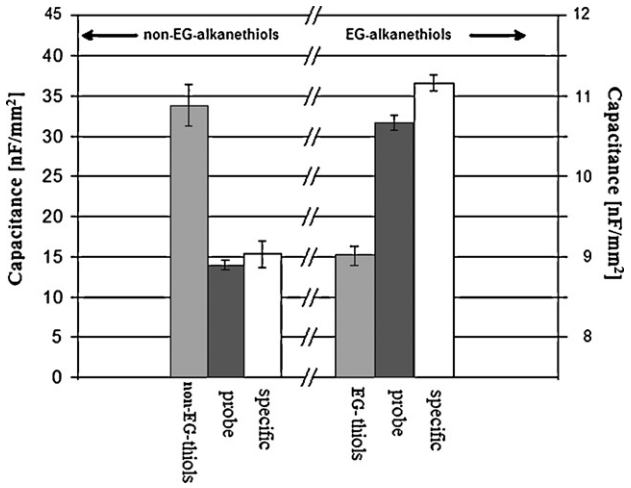

Fig. 2. Capacitance measurements acquired on thiols film, probe IgG molecules, and on incubated specific antigen molecules (SCCA–Hepatocarcinoma marker). The comparison is between the usually considered IgG probes immobilization technique by using 11-mercaptoundecanoic acid (data on the left) and the new technique proposed in this paper based on IgG antibodies covalently bound to ethylene–glycol alkanethiols monolayer (right data). The reported data errors are calculated as three times the standard deviation in measurement series acquired upon the time on the same chip spot. The errors correspond to the 99% of statistical data significance. All the measurements were carried out in PBS buffer.

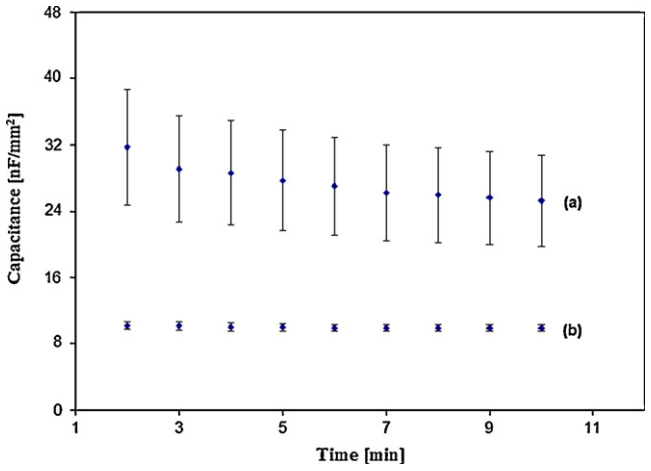

Fig. 3. Time trends of capacitance measurements acquired on films of alkanethiol without (a) and with (b) ethylene–glycol functionalization. All the measurements were carried out in PBS buffer. Error bars represent in-chip reproducibility (reproducibility spot-by-spot on the same chip).

EG-alkanethiols. Fig. 2 compares the behaviour of IgG immobilized onto a film prepared by using 11-mercaptoundecanoic acid and IgG immobilized on a film prepared by using EG-alkanethiols. A decreasing capacitance is observed in DNA target detection in the graphs presented in Fig. 1. Similar decrease is also observed after antibodies immobilization onto non-EG-alkanethiols in Fig. 2. A capacitance decrease is coherent with the phenomena of ions displacement from the electrode surface (Mirsky et al., 1997; Berggren et al., 1999). However, capacitance increase was observed after molecules immobilization onto EG-alkanethiols films, both in case of DNA (Fig. 1) and antibodies (Fig. 2). A further increase in capacitance upon antigen detection was a common feature in all of our measurements with EG-alkanethiols surfaces. Capacitance decrease after proteins incubation was only observed with IgG immobilized onto non-EG-alkanethiols (Fig. 2), as previously observed in similar experiments on antibodies against interleukins (Berggren et al., 1998). Capacitance decreases in this case because a conducting aqueous solution is being replaced by a hydrophobic protein. Capacitance changes because additional proteins fill up unoccupied sites displacing some of the diffuse layers further out into solution (Berggren et al., 1998). The hydrophobicity of long alkyl chains is well known (Smith and Tanford, 1973), while there is much stronger coordination of water molecules close to the ethylene–glycol chains (Ostumi et al., 1999). On the EG-alkanethiols surface, a capacitance increase was observed every time after molecules incubation, both for proteins and for DNA probes. A slight increase was also observed on EG-alkanethiols in case of un-specific DNA binding (Fig. 1, bars triple on the right). This means that the signal change is due to net molecule charge contribution and not to solution ions displacement. On the other hand, the obtained capacitance values are coherent with those obtained by other authors in terms of measured capacitance per unit area. We measured 4 $\mu F/cm^2$ on 11-mercaptoundecanoic acid monolayers which is within the range already measured for these films (from 3 to 9 $\mu F/cm^2$, published by Riepl et al., 1999). We measured a capacitance of 9 nF/mm^2, e.g. 0,9 $\mu F/cm^2$, on EG-alkanethiols, which is one order of magnitude less, coherently with a longer molecular chain. We also measured a capacitance in the range of 8–11 nF/mm^2 for the IgG and in the range of 4–6 nF/mm^2 for the ssDNA both immobilized onto EG-alkanethiols. It was in the range 10–12 nF/mm^2 for the antigen (SCCA–hepatocarcinoma marker) and in the range of 4–6 nF/mm^2 for the target DNA. The registered variations in the SCCA detection are close to 1 nF/mm^2, which is 100 nF/cm^2. This value is in the same range of 30–130 nF/cm^2 recently obtained in alpha-fetoproteins detection (Limbut et al., 2006). Our detection percentage errors are in the range of 11–37% and 0,23–0,82% for antigen and DNA, respectively. The in-chip reproducibility (reproducibility spot by spot on the same chip) is in the range of 10–22%. The average standard deviation of different measurements in time on the same chip's spot is close to 0,44% for the EG-alkanethiols, to 1% for DNA probes and targets, and close to 7% for antibody and antigen surfaces.

3.2. Capacitance Time Drift and AFM Images

The antigen detection was not statistically significant in our experiments with IgG immobilized onto non-EG-alkanethiols (Fig. 2) due to large time drift and to capacitance measurement errors (Fig. 3, curve 'a'). The decreasing time drift registered with non-EG-alkanethiols is similar to trends usually registered on clean gold bare electrodes. Similar time drifts were also registered with films directly immobilized onto gold electrodes and made by thiols (Mirsky et al., 1997; Riepl et al., 1999), GST proteins (Corbisier et al., 1999), phytochelatine (Bontidean et al., 2003), PNA (Macanovic et al., 2004), and DNA (Stagni et al., 2006). Instead, the acquired capacitances became highly stable in time if probe molecules were immobilized onto anchoring monolayers prepared with EG-alkanethiols (Fig. 3, curve 'b'). The improved time behaviour also results in a higher reproducibility. With antibodies onto EG-alkanethiols, we registered electrode-to-electrode reproducibility of 10–22% in the same chip and measurement errors close to 0,44% in time series in the same spot. The reason of this improvement is on the film quality. On the other hand, previous experiments with antibodies immobilized onto non-EG-alkanethiols showed electrode-to-electrode reproducibility equal to 30–40% (Berggren et al., 1998). Fig. 4(A) and (B) show that the film quality is highly different in case of films made by using non-EG-alkanethiols or EG-alkanethiols. The estimated depth of grooves shown in Fig. 4(A) is even larger than that usually expected from the theoretical film height. Similar discrepancies were already observed (Franzen, 2003). Such an apparent increase in film's height may be due to the hydrogenated alkane part of the molecules (Ichii et al., 2005) and a quantitative comparison between the friction forces of different

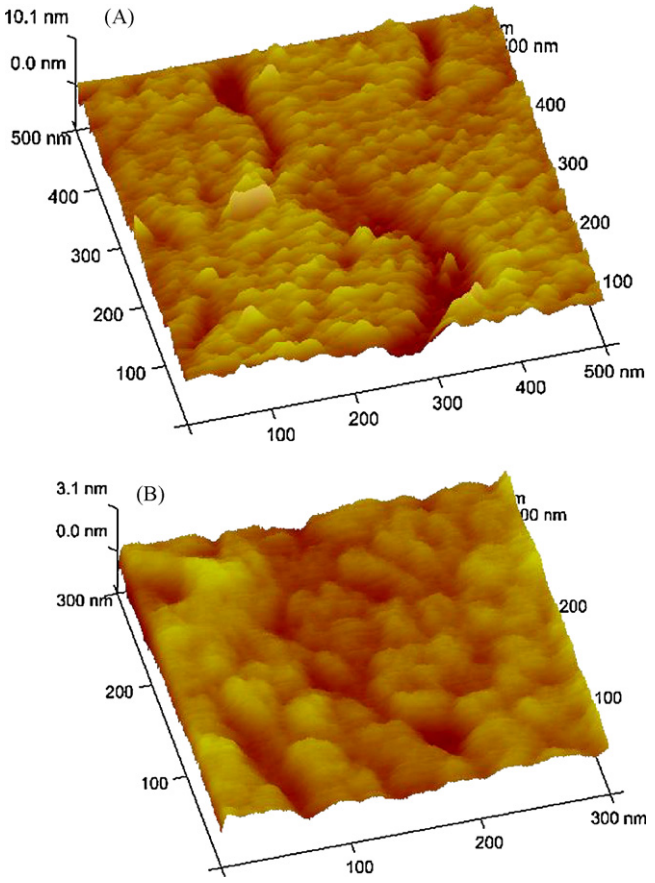

Fig. 4. AFM images acquired on alkanethiols without ethylene–glycol functionalization (A) and with ethylene–glycol functionalization (B). The images show that grooves with depths comparable with the film thickness are present in the first case while grooves are totally absent and surface is smooth in the second case. The images were acquired in liquid conditions. The liquid was ethanol, as in case of self-assembly films formation.

systems from image average corrugations is questionable (Ohzono and Fujihira, 2000). Moreover, it is well known that the required *Q* factor of AFM tips needs to be smaller than few hundred in order to achieve true-molecular resolution (Fukuma et al., 2005). Nevertheless, grooves crossing the whole film can be deduced from AFM imaging on thin molecular films (Bavastrello et al., 2004). Thus, we conclude that grooves in our non-EG-alkanethiol films are crossing the whole monomolecular thickness. In other hand, films prepared with EG-alkanethiol molecules have shown small surface corrugation and absence of deep grooves (Fig. 4(B)). The average film corrugation estimated by image analysis (Carrara et al., 2000) is $0{,}8 \pm 0{,}1$ nm for EG-alkanethiols, which is not so far from that of 0,3 nm for a bare TSG (Medalia et al., 2002). It is much higher ($1{,}3 \pm 0{,}3$ nm) in case of films made with non-EG-alkanethiols and single image's lines may present groves which are deep up to 3 nm. Images on films without ethylene–glycol functionalization present sharp features while those on ethylene–glycol films are smoother. Also this fact is connected to different wettability of the monolayers. Infrared spectroscopy demonstrates that ethylene–glycol chains in methoxy-terminated monolayer are mainly in great disorder, while they are in a crystalline helical phase in hydroxyl-terminated monolayer (Harder et al., 1998). *Ab initio* calculations showed that the energetic of water adsorption in EG-films is dominated by electrostatic interactions and that helical conformation of ethylene–glycol chains adsorbs water molecules better than planar conformation (Wang et al., 1997). We have a large amount of hydroxyl-terminated EG-alkanethiols in our films. So, we expected a strong coordination of water molecules in our ethylene–glycol chains (as schematically reported in drawing (C) of on-line available Supplementary file # 1). By using QCM, we observed an increase in the film's mass in dry measurements after conditioning in pure Milli-Q water. We estimated the water amount trapped into molecular film. The dried film mass shows a variation of 0,14 ng/mm^2 after 1 h of water conditioning. The estimated mass change corresponds to 16 water molecules for each organic molecule. It is also known that hydrophobic chains can retain few water molecules when the films are dried (Carrara et al., 2000). Thus, up to 7 water molecules for each organic molecule may be stored in dried alkyl chains film (Carrara et al., 2000), while the other water molecules are strongly coordinated by ethylene–glycol chains. This water content that deeply bounds to the film is the reason of the improved smoothness of the monolayer as observed in AFM imaging. Our AFM imaging has shown more corrugated pictures with deep defects in the monolayer for non-EG-alkanethiols films. In these films, the absence of ethylene–glycol chains coordinating water molecules allows a deeper penetration of the AFM tip into the molecular film. Similar deep defects were also found on STM images acquired on thiols with long alkyl and without ethylene–glycol components (Sun and Crooks, 1991). The idea of a key role for the water in the film behaviour was also confirmed by the improved electrical behaviour of films after water conditioning. The conditioning results in a further stabilization of interfacial capacitance. Stabilization is due to a strong correlation of the solvated ions surrounding ethylene–glycol chains which are reorganized in a very compact and crystalline helical conformation. After equilibration, ethylene–glycol function significantly improves the electrode polarization because these groups form an ordered hydrated layer that prevents solution ions to reach the electrode surface. In this manner, electron transfer between solution and gold electrode is not possible. The presence of deep groves reported by AFM images is a direct proof that gold electrode surface is accessible to solution ions in films prepared by using non-EG-alkanethiols (as schematically shown by drawings available on-line in Supplementary file # 1). These grooves represent free pathways for buffer ions to electrode surface. Therefore, a not well packed thiols and DNA monolayer allow buffer ions to reach electrodes surface. Instead, a well packed and well hydrated film prepared by using the EG-alkanethiols shows very stable capacitance values (Fig. 3, curve 'b') and do not presents deep groves in AFM images (Fig. 4(B)).

3.3. QCM Measurements and Detection Efficiency

Surface densities were estimated by using QCM and results were summarised in Table 1. The obtained values of surface densities are in good agreement with data already published on similar systems (for a direct comparison, see Table 2 reported in on-line available in Supplementary file # 2). In fact, a surface density equal to 0,28 ng/mm^2 was reported in case of 11-mercapto-undecanoic acid SAM monolayer (Keselowsky et al., 2003). A number of molecules in the order of 10^{13} molecules/cm^2 have been reported in literature for DNA probe molecules estimated by optical measurements (Stagni et al., 2007; Yoon-Kyoung Cho et al., 2004). Our estimation on DNA molecules is lower. It is in the range of 10^{12} molecules/cm^2. This is because we immobilize lesser amounts of DNA probe molecules; the ratio between COOH anchoring groups and OH repelling groups on top of our EG-alkanethiols film is 1:50. A density equal to 6×10^9 molecules/mm^2 was reported for IgG investigated by SPR (Teramura Yuji et al., 2006). It is close to our estimation value. Our surface density for antibodies is in the range from 0,62 to 1,13 ng/mm^2 reported for different antibody types (Bonroy et al., 2006). Theoretical calculations for highly packed IgG layers range from 1,3 to 6,5 ng/mm^2 (Bonroy et al., 2006) and antibodies cover-

Table 1
QCM measurements estimated as surface mass density and density of molecules number for EG-alkanethiols and the immobilized probes molecules.

	EG-alkanethiols	DNA probes	IgG probes
Surface density [ng/mm^2]	0,23 ± 0,05	0,17 ± 0,01	0,81 ± 0,01
# of molecules [molecules/mm^2]	$3{,}0 \times 10^{11}$	$5{,}9 \times 10^{10}$	$3{,}6 \times 10^{9}$

age could be improved up to 4,48 ng/mm^2 by using glutaraldehyde (Fireman et al., 2007). However, the increase in antibodies coverage may result in a decrease in the binding efficiency due to steric hindrance (Vikholm et al., 1998). Our antigen binding efficiency is equal to 47%, a value which compares quite well with the 67% obtained in QCM experiments on IgG fragments immobilized onto lipid matrixes (Vikholm et al., 1998). These values are much larger than 5,8% estimated by RIE (Vikholm et al., 1998) or 9% estimated by SPR (Teramura Yuji et al., 2006) and obtained with other immobilization techniques.

4. Conclusions

The originality of this paper is the identification of a surface functionalization which drastically reduces time drift of interface impedance and, therefore, enhances DNA and antigen detection via capacitance measurements. We described a new protocol to immobilize both single strand DNA and IgG probe molecules onto capacitive bio-chip by means of COOH-terminated ethylene–glycol alkanethiols. Capacitance measurements were analyzed in time domain. It has been proved that the sensing surfaces prepared with ethylene–glycol functional groups present electrochemical behaviour close to that of a stable capacitor. The improved stability of these surfaces was explained in terms of ions pathways absence into the sensing surface and of water organization. This theory was demonstrated by showing the presence of such pathways in AFM images of alkanethiol films without ethylene–glycol functional groups. In contrast, AFM images on ethylene–glycol films do not present grooves and they show highly packed structures with a surface corrugation not larger than that expected for the substrate. The presence of a stable water layer close to ethylene–glycol chains was directly confirmed by QCM experiments. This interfacial behaviour ensures improved detection capability. The optimized behaviour due to the new functionalization has lead to very small standard deviation in capacitance data of chip spots. In conclusion, we have demonstrated that ethylene–glycol alkanethiols are highly suitable and reliable materials for applications in label-free capacitance detection of biomolecules.

Acknowledgments

S.C. and V.B. thank Francesco Valle for his support in AFM imaging. Olivetti I-jet is gratefully acknowledged for designing and fabricating the used bio-chips. Anil Leblebici is acknowledged for English revision of the paper. The research has been financially supported by the European Project FP6 DINAMICS and by the Italian national project FIRB entitled “Nanosized Cancer Polymarker Biochip” (code RBLA03S4SP).

Appendix A. Supplementary data

Supplementary data associated with this article can be found, in the on-line version, at doi:10.1016/j.bios.2008.11.014.

References

Balasubramanian, A., Bhuva, B., Mernaugh, R., Haselton, F.R., 2005. IEEE Sens. J. 1530–437, 1–5.
Bavastrello, V., Erokhin, V., Carrara, S., Sbrana, F., Ricci, D., Nicolini, N., 2004. Thin Solid Films 468, 17–22.
Berggren, C., Stalhandske, P., Brundell, J., Johnansson, G., 1999. Electroanalysis 11, 156–160.
Berggren, C., Bjarnason, B., Johnansson, G., 1998. Biosens. Bioelectron. 13, 1061–1068.
Berggren, C., Johansson, G., 1997. Anal. Chem. 69, 3651–3657.
Berggren, C., Bjarnason, B., Johansson, G., 2001. Electroanalysis 13, 173–180.
Betty, C.A., Lal, R., Sharma, D.K., Yakhmi, J.V., Mittal, J.P., 2004. Sens. Actuators B 97, 334–343.
Bonroy, K., Frederix, F., Reekmans, G., Dewolf, E., De Palma, R., Borghs, G., Declerck, P., Goddeeris, B., 2006. J. Immunol. Methods 312, 167–181.
Bontidean, I., Ahlqvist, J., Mulchandani, A., Chen, W., Bae, W., Mehra, R.K., Mortari, A., Csoregi, E., 2003. Biosens. Bioelectron. 18, 547–553.
Carrara, S., Erokhin, V., Nicolini, C., 2000. Langmuir 16, 6577–6582.
Carrara, S., Gürkaynak, F.K., Guiducci, C., Stagni, C., Benini, L., Leblebici, Y., Samorì, B., De Micheli, G., 2007. Sens. Trans J. 76, 969–977.
Carrara, S., Bhalla, V.K., Stagni, C., Benini, L., Riccò, B., Samorì, B., 2008. Sens. Trans. J. 88, 31–39.
Corbisier, P., Van der Lelie, D., Borremans, B., Provoost, A., De Lorenzo, V., Brown, N.L., Lloyd, J.R., Hobman, J.L., Csoregi, E., Johansson, G., Mattiasson, B., 1999. Anal. Chim. Acta 387, 235–244.
Daniels, J.S., Pourmand, N., 2007. Electroanalysis 19, 1239–1257.
Facci, P., Erokhin, V., Nicolini, C., 1993. Thin Solid Films 230, 86–89.
Fireman, R., Dutra, R., Mendes, K., Lins da Silva, V., Tatsuo Kubot, L., 2007. J. Pharm. Biomed. Anal. 43, 1744–1750.
Franzen, S., 2003. Chem. Phys. Lett. 381, 315–321.
Fukuma, T., Ichili, T., Kobayashi, K., Yamada, H., Matsushige, K., 2005. Appl. Phys. Lett. 86 034103-1, 3.
Guiducci, C., Stagni, C., Zuccheri, G., Bogliolo, A., Benini, L., Samorì, B., Riccò, B., 2004. Biosens. Bioelectron. 19, 781–787.
Harder, P., Grunz, M., Dahint, R., Whiteside, G.M., 1998. J. Phys. Chem. B 102, 426–436.
Horan, N., Lin, Yan, Isobe, H., Whitesides, G.M., Kalne, D., 1999. Proc. Natl. Acad. Sci. U.S.A. 96, 11782–11786.
Keselowsky, B.G., Collard, D.M., García, A.J., 2003. J. Biomed. Mater. Res. 66A, 247–259.
Ichii, T., Urabe, M., Fekema, T., Kobayashi, K., Matsushige, K., Yamada, H., 2005. Japanese J. Appl. Phys. 44, 5378–5381.
Jae Hyun, Jeong, Byoung Yun, Kim, Seung Jun, Lee, Jong-Duk, Kim, 2006. Chem. Phys. Lett. 421, 373–377.
Lahiri, J., Isaacs, L., Tien, J., Whitesides, G.M., 1999. Anal. Chem. 71, 777–790.
Limbut, W., Kanatharana, P., Mattiasson, B., Asawatreratanakul, P., Thavarungkul, P., 2006. Biosens. Bioelectron. 22, 233–240.
Gabig-Ciminska, M., 2006. Microb. Cell Factories 5, 1–8.
Macanovic, A., Marquette, C., Polychronakos1, C., Lawrence, M.F., 2004. Nucleic Acids Res. 32, 1–7.
Medalia, O., Englander, J., Guckenberger, R., Sperling, J., 2002. Ultramicroscopy 90, 103–112.
Mirsky, V.M., Riepl, M., Wolfbeis, O.S., 1997. Biosens. Bioelectron. 12, 977–989.
Ohzono, T., Fujihira, M., 2000. Phys. Rev. B 62, 17055–17071.
Ostumi, E., Yan, Lin, Whitesides, G.M., 1999. Colloids Surf. B: Biointerf. 15, 3–30.
Rickert, J., Brecht, A., Göpel, W., 1997. Biosens. Bioelectron. 7, 567–575.
Riepl, M., Mirsky, V.M., Novotny, I., Tvarozek, V., Rehacek, V., Wolfbeis, O.S., 1999. Anal. Chim. Acta 392, 77–84.
Smith, R., Tanford, C., 1973. Proc. Natl. Acad Sci. U.S.A. 70, 289–293.
Stagni, C., Guiducci, C., Benini, L., Riccò, B., Carrara, S., Samorí, B., Paulus, C., Schienle, M., Augustyniak, M., Thewes, R., 2006. IEEE J. Solid-State Circuits 41, 2956–2964.
Stagni, C., Guiducci, C., Benini, L., Riccò, B., Carrara, S., Paulus, C., Schienle, M., Thewes, R., 2007. IEEE Sens. J. 7, 577–585.
Sun, L., Crooks, R.M., 1991. J. Electrochem. Soc. 138, L23–L25.
Teramura, Yuji, Yusuke, Arima, Hiroo, Iwata, 2006. Anal. Biochem. 357, 208–215.
Vikholm, I., Albers, W.M., Välimäki, H., Helle, H., 1998. Thin Solid Films 327–329, 643–646.
Yoon-Kyoung, Cho, Sunhee, Kim, Young A., Kim, Hee Kyun, Lim, Kyusang, Lee, Dae-Sung, Yoon, Geunbae, Lim, Eugene Pak, Y., Tai Hwan, Ha, Kwan, Kim, 2004. J. Colloid Interf. Sci. 278, 44–52.
Wang, R.L.C., Kruezer, H.J., Grunz, M., 1997. J. Phys. Chem. B 101, 9767–9773.